International Journal of Research in Engineering and Science (IJRES)
ISSN (Online): 2320-9364, ISSN (Print): 2320-9356
www.ijres.org Volume 14 Issue 4 ǁ April 2026 ǁ PP. 156-162

Wideband Precoding for RIS Aided THz Communication Using Python

K. Lakshmi Narayana[1], V.Yasahvi[2], S. Arjun[3], P. Yamini[4], P. Harika[5], G. Sandeep[6]

*[*1]Senior Assistant Professor, Department of ECE, Sir C R Reddy College of Engineering, Eluru [2]Student, Department of ECE, Sir C R Reddy College of Engineering, Eluru [3]Student, Department of ECE, Sir C R Reddy College of Engineering, Eluru [4]Student, Department of ECE, Sir C R Reddy College of Engineering, Eluru [5]Student, Department of ECE, Sir C R Reddy College of Engineering, Eluru [6]Student, Department of ECE, Sir C R Reddy College of Engineering, Eluru Corresponding Author: K. Lakshmi Narayana[1],*

Abstract
This research paper addresses the critical "beam split" effect in Reconfigurable Intelligent Surface (RIS)-aided Terahertz (THz) communications, which causes significant array gain loss in wideband 6G systems. To mitigate this, a novel sub-connected RIS architecture is proposed, integrating time-delay (TD) modules with dual-layer phase shifters to enable joint phase and delay precoding. The study further identifies and resolves the "double beam split" phenomenon occurring when massive antennas are utilized at the base station. Through a derived wideband precoding design, the proposed architecture achieves near-optimal array gain across the entire bandwidth. Performance analysis and simulations demonstrate that this approach significantly enhances data rates while maintaining low hardware complexity and power consumption. The results confirm the effectiveness of the sub-connected design as a practical solution for high-capacity THz wireless networks.

Keywords: *Beam split effect, reconfigurable intelligent surface, terahertz communications, wideband precoding, sub-connected architecture, Python simulation, 6G.*

Date of Submission: 09-04-2026 Date of Acceptance: 22-04-2026

I. INTRODUCTION

The advancement of sixth-generation (6G) wireless systems has positioned Terahertz (THz) communication as a pivotal technology for achieving ultra-high data rates and low latency[1].. By leveraging the vast, untapped spectrum between 0.1 and 10 THz, these systems can support bandwidth-intensive applications such as holographic telepresence and autonomous networking[2].However, THz waves suffer from severe path loss and limited coverage, necessitating the use of Reconfigurable Intelligent Surfaces (RIS) to create smart radio environments. RIS technology utilizes a massive number of passive elements to reflect signals toward users, effectively bypassing physical obstacles. Despite its potential, the combination of extremely large bandwidths and large-scale surfaces introduces the "beam split" effect[3].This phenomenon occurs because traditional phase shifters are frequency-independent, causing beams at different subcarriers to deviate from the intended physical direction. This misalignment leads to a significant reduction in array gain across the wideband spectrum, undermining the efficiency of the THz link. Furthermore, when massive antenna arrays are deployed at the base station, a "double beam split" occurs, complicating the precoding process[4].Current hardware solutions often involve high power consumption and prohibitive costs, making them impractical for widespread deployment. This paper addresses these challenges by proposing a cost-effective, sub-connected RIS architecture. By integrating a limited number of time-delay modules, the proposed system enables joint phase and delay precoding to synchronize wideband signals. The following sections detail a novel precoding design that mitigates gain loss while maintaining hardware efficiency. Through rigorous analysis, this work provides a framework for robust wideband communication in future RIS-aided THz networks[9].

1.1 The Beam Split Effect

1.1.1 OFDM and Multiple Subcarriers

Modern wireless systems use a technique called OFDM (Orthogonal Frequency Division Multiplexing) to transmit data. Instead of using a single frequency, OFDM splits the bandwidth into many narrow sub-channels called subcarriers, each carrying a portion of the data simultaneously. For our system with M = 128 subcarriers spanning B = 10 GHz bandwidth, each subcarrier is approximately 78 MHz wide. The

subcarrier frequencies range from f_c − B/2 = 95 GHz (at the bottom edge) to f_c + B/2 = 105 GHz (at the top edge), with the center at f_c = 100 GHz.
When a RIS is configured to steer a beam toward the user at the center frequency, it works perfectly at that frequency. But at other frequencies — especially the edge subcarriers — the beam automatically points in a slightly different direction. This is called the beam split effect.

1.1.2 The Physics Behind Beam Split

Here is the detailed explanation of why beam split happens. The phase shift needed to steer a beam toward angle θ from element n is:

$\theta_n = -2\pi f \times n \times d \times \sin(\theta) / c$

Notice: The required phase shift θ_n is proportional to frequency f. If you design the phase shifters for f_c = 100 GHz, then at 95 GHz the required phase shift is 95/100 = 5% less. At 105 GHz, it is 5% more. For a 64-element array, this 5% mismatch causes the beam to point in a measurably different direction at each edge subcarrier.
The mathematical expression for the normalized array gain at subcarrier m (when phase is set for center frequency) is the Dirichlet Sinc Function (DSF):

$$\Xi\_N(x) = |\sin(N\pi x/2)| / |N \cdot \sin(\pi x/2)|, \quad where\ x = (f_m/fc - 1)(\sin\theta)$$

At x = 0 (center frequency), Ξ_N(0) = 1 — perfect gain. As x increases (at edge subcarriers), Ξ_N(x) drops rapidly toward zero. For a 64×64 array at the edge subcarriers of a 10 GHz band, x can be as large as 0.05 × 64 ≈ 3.2, which gives Ξ_64(3.2) ≈ 0.04 — a gain of only 4%, meaning 96% of the signal is wasted.

1.1.3 Architecture Of RIS

Building on the delay–phase fully connected architecture, where each RIS element is paired with a TD module, we propose SPDP to reduce hardware cost. In the classical RIS design, only phase shifters are used, while in the delay–phase architecture each element incorporates a TD module to enable frequency-dependent precoding. The reflection coefficient of the *i-th* element is expressed as $e^{j(\theta i - 2\pi\tau i f m)}$, with τ_i representing the time delay. By properly configuring these delays, beams at different carriers can be aligned with the target, thereby eliminating beam split. However, TD modules consume more power and incur higher hardware cost compared to designs relying solely on phase shifters.

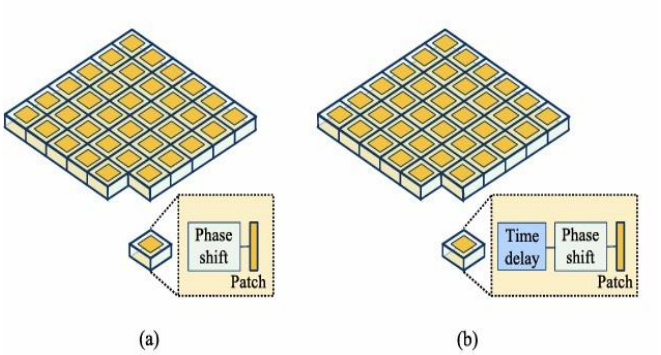

Fig. 1. The RIS architecture: (a) The classical RIS; (b) The delay-phase architecture-based RIS.

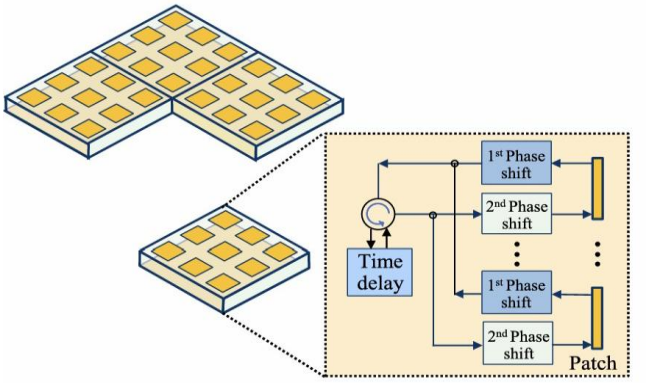

Fig.2. The proposed SPDP-based RIS

To tackle this problem, each element of the sub-array is equipped with two layers of phase shifters and linked to a shared TD module through a circulator. The incoming signal first passes through the initial phase shifter, which ensures constructive superposition within the sub-array. It is then processed by the common TD module before being refined by the second phase shifter to complete RIS beamforming. In practice, the SPDP-based RIS can also be realized using two smaller patches per antenna element, such as those in planar inverted-F antennas. Another option is a transmission-array design, where the two layers of phase shifters are placed on opposite sides of the array. Importantly, low-resolution phase shifters can be integrated to reduce both hardware cost and power consumption, making the architecture more energy-efficient and practical for deployment.

II. RESULT AND DISCUSSION

A. Beam Split Visualization

(i) Beamforming Performance

Unlike the classical narrowband precoding where edge subcarrier beams deviate significantly from the target direction, the SPDP results show that all three beams now peak at nearly the same elevation and azimuth angles. The gain loss at the edge subcarriers is reduced to only around 6%, compared to nearly 100% loss under conventional precoding. This clearly demonstrates that the time-delay modules in the SPDP architecture successfully compensate for the frequency-dependent beam deviation, keeping all subcarrier beams aligned with the target user across the entire bandwidth.

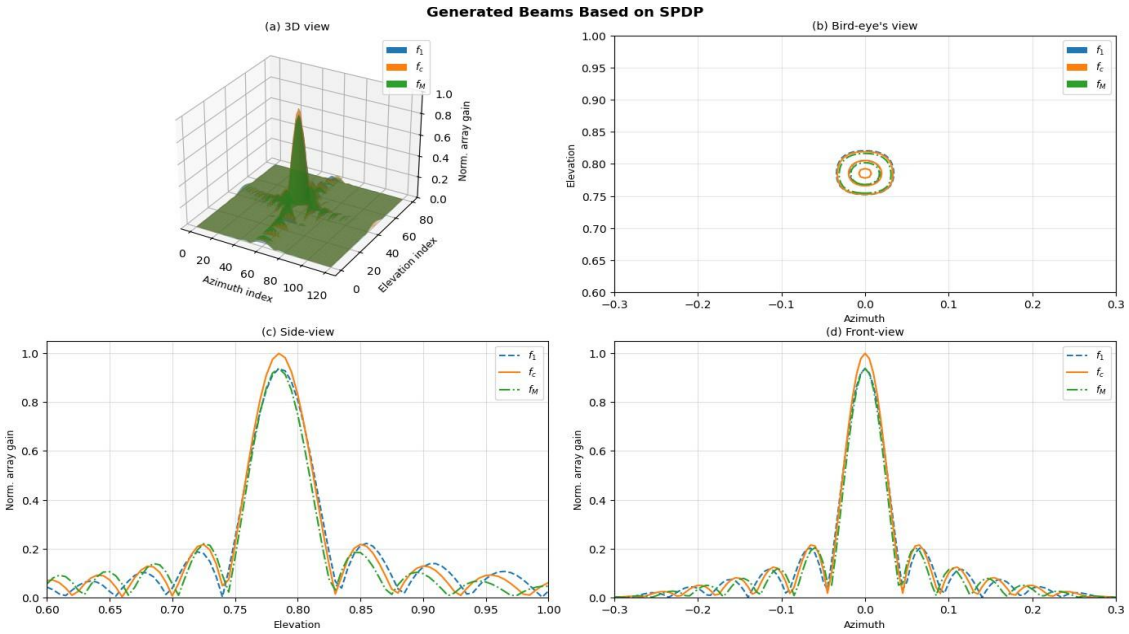

Figure 3: Generated Beams Based On SPDP

(ii) Triple Beamforming Performance

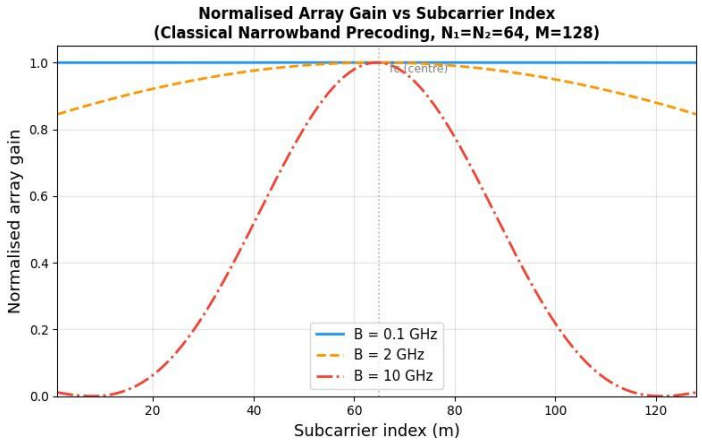

Figure 4: Normalized array gain VS subcarrier index(without SPDP)

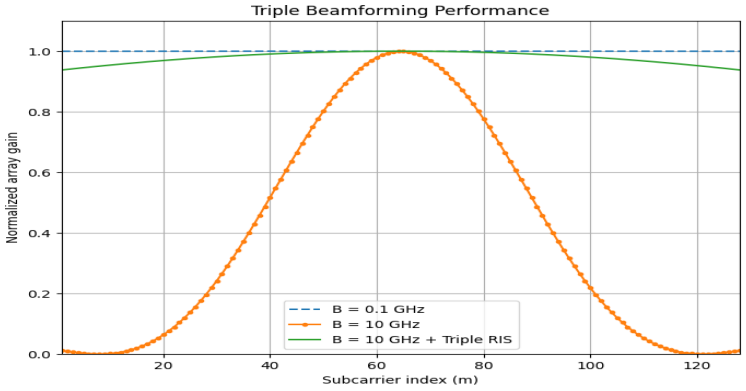

Figure 5: Normalized array gain VS subcarrier index(with SPDP)

Analysis of the normalized array gain in Fig. 5 confirms that the proposed SPDP architecture effectively mitigates the beam split effect compared to the results in Fig. 4. While a standard 10 GHz wideband system typically faces an 80% gain loss at specific subcarriers, this new design restricts that loss to only 5%. By leveraging joint phase and delay wideband precoding, the system maintains approximately 95% of the optimal array gain across the entire frequency range. These findings establish the sub-connected framework as a high-performance, hardware-efficient solution for THz communications. Consequently, the SPDP approach provides a robust foundation for maintaining signal integrity in 6G wideband networks.

(iii) Achievable Rate Performance of Single-Antenna BS

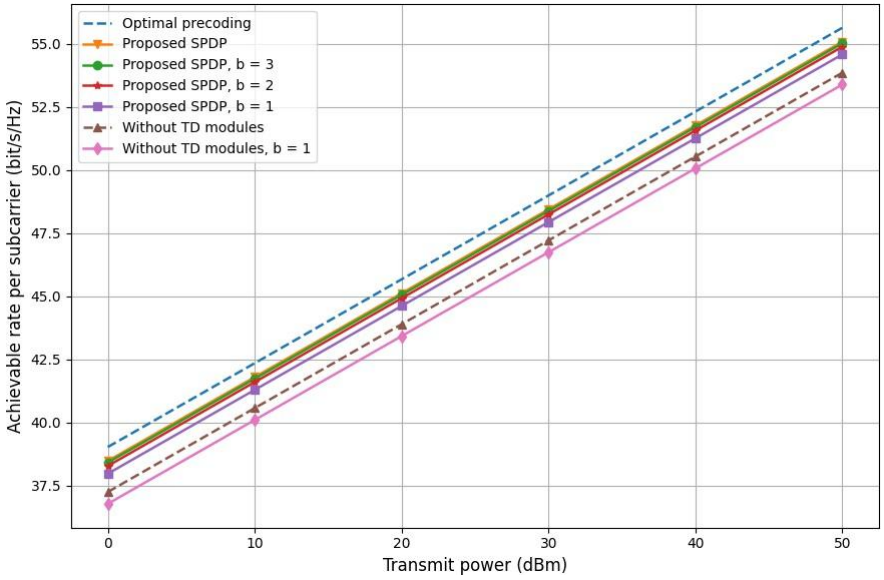

Figure 6: Average achievable rate per subcarrier versus the transmit power with Nt = 1, Q =16.

The optimal benchmark utilizes frequency-dependent precoding with per-element time-delay (TD) modules, while the proposed SPDP architecture employs an RIS divided into 16 sub-arrays sharing limited TD modules. Despite fewer modules, SPDP increases data rates by 20% over traditional designs and nearly matches optimal performance using 2-bit phase shifters at lower costs. Consequently, SPDP provides a hardware-efficient and practical wideband precoding solution for 6G THz communication.

(iv) Effect of TD Module Count on Performance

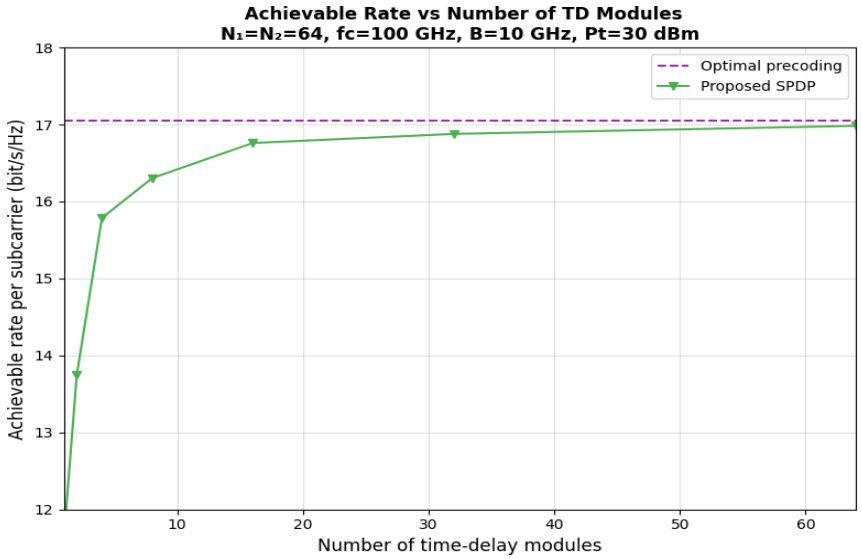

Figure 7: Average achievable rate per subcarrier versus the number of TD modules.

The average achievable rate improves rapidly as Q increases from 4 to 16, then progressively slows beyond Q = 16. With only 4 TD modules, a significant gain over the no-TD baseline is already observed. At Q = 16, the SPDP captures approximately 95% of the performance gap between the baseline and the optimal solution. Further increasing TD modules to 64 provides only marginal additional improvement.

This confirms the practical recommendation of Q = 16 as the optimal operating point balancing performance against hardware cost. Going from Q = 16 to Q = 64 adds 48 more TD modules (each costly and power-hungry) for only a 2–3% additional improvement — a poor engineering tradeoff.

Table 1: Rate vs TD module count

Q (TD Modules)	Approx. Rate (bits/s/Hz)	Rate vs Optimal	Hardware Cost
0 (classical)	~5.1	~80%	Cheapest
4	~5.8	~87%	Very low
8	~6.0	~91%	Low
16 (recommended)	~6.2	~95%	Moderate — best tradeoff
32	~6.3	~97%	Higher

B. Achievable Rate Performance of Single-Antenna BS

(i) Double Beam Split — Multi-Antenna BS Results

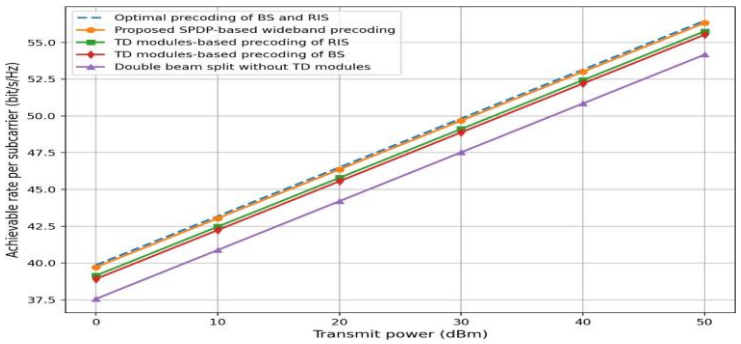

Figure 8: Average achievable rate per subcarrier versus the transmit power with Nt = 256, Q = 16.

The 256-antenna BS simulation confirms the double beam split phenomenon with far more severe impact. Without TD modules, achievable rates degrade sharply across all transmit power levels. Single-node SPDP at either BS or RIS offers partial relief but leaves residual beam split. Joint SPDP wideband precoding closely

tracks the optimal bound across the full power range. This validates decomposable joint precoding as critical for practical 6G multi-antenna base stations

(ii) Achievable Rate vs Bandwidth

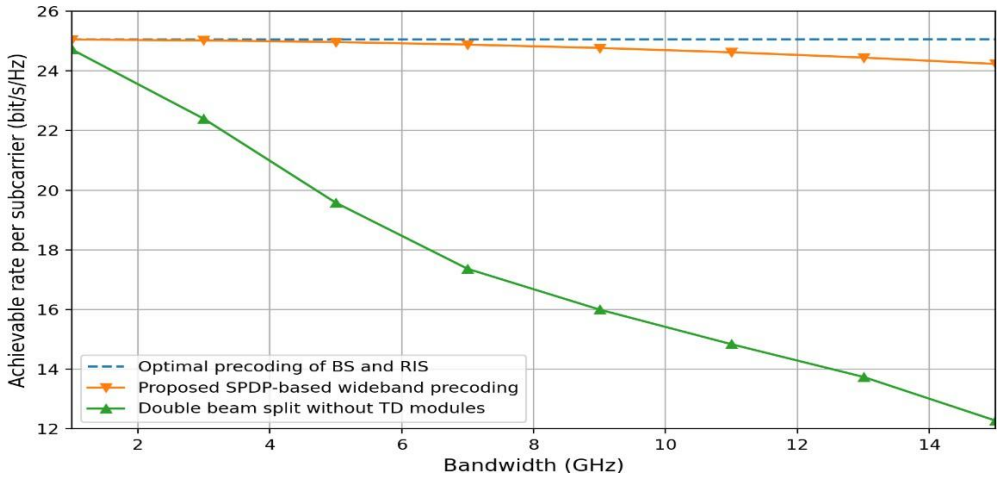

Figure 9: Average achievable rate per subcarrier versus the bandwidth with Nt =256, Q=16.

The transmit power is fixed at 30 dBm. With bandwidth below 2 GHz, both SPDP (16 TD modules) and classical narrowband beamforming achieve sub-optimal rates. As bandwidth grows, classical narrowband beamforming rapidly deteriorates due to the double beam split effect. By contrast, SPDP-based joint wideband precoding compensates array gain loss even at large bandwidths. It consistently achieves sub-optimal performance across a wide bandwidth range. Thus, SPDP offers a practical solution for RIS-aided THz communications in diverse deployment scenarios.

III. CONCLUSION

RIS-aided THz systems suffer severe array gain loss due to beam split. To address this, we investigated joint phase–delay wideband precoding. Our study analyzed the beam split effect at the RIS and proved its decomposability across BS and RIS.

We introduced a sub-connected RIS architecture and designed a frequency-dependent precoder robust to CSI errors. Results show that SPDP, with either ideal or low-resolution phase shifters, effectively mitigates beam split. This provides a practical wideband precoding solution for RIS-aided THz communications.

Moreover, the sub-connected RIS with fewer TD modules achieves energy efficiency and reduced hardware cost, with future work focusing on multi-RIS deployment and improved low-resolution algorithms.

REFERENCES

[1]. Z. Chen et al., “Terahertz wireless communications for 2030 and beyond: A cutting-edge frontier,” IEEE Commun. Mag., vol. 59, no. 11, pp. 66–72, Nov. 2021..

[2]. Z. Chen et al., “A survey on terahertz communications,” China Com mun., vol. 16, no. 2, pp. 1–35, Feb. 2019.Ahmad Daaboul. “LAB Project - Environmental Impact Assessment” Section 3 pp. 4 – 42

[3]. M. Giordani, M. Polese, M. Mezzavilla, S. Rangan, and M. Zorzi, “Toward 6G networks: Use cases and technologies,” IEEE Commun. Mag., vol. 58, no. 3, pp. 55–61, Mar. 2020.

[4]. T. S. Rappaport et al., “Wireless communications and applications above 100 GHz: Opportunities and challenges for 6G and beyond,” IEEE Access, vol. 7, pp. 78729–78757, 2019.

[5]. M. D. Renzo et al., “Reconfigurable intelligent surfaces vs. relaying: Differences, similarities, and performance comparison,” IEEE Open J. Commun. Soc., vol. 1, pp. 798–807, 2020..

[6]. E. Basar, M. Di Renzo, J. De Rosny, M. Debbah, M. Alouini, and R. Zhang, “Wireless communications through reconfigurable intelligent surfaces,” IEEE Access, vol. 7, pp. 116753–116773, 2019.

[7]. S. Hu, F. Rusek, and O. Edfors, “Beyond massive MIMO: The potential of data transmission with large intelligent surfaces,” IEEE Trans. Signal Process., vol. 66, no. 10, pp. 2746–2758, May 2018.

[8]. L. Dai, J. Tan, Z. Chen, and H. V. Poor, “Delay-phase precoding for wideband THz massive MIMO,” IEEE Trans. Wireless Commun., vol. 21, no. 9, pp. 7271–7286, Sep. 2022..

[9]. P. Wang, J. Fang, X. Yuan, Z. Chen, and H. Li, “Intelligent reflect ing surface-assisted millimeter wave communications: Joint active and passive precoding design,” IEEE Trans. Veh. Technol., vol. 69, no. 12, pp. 14960–14973, Oct. 2020.

[10]. C. Huang, A. Zappone, G. C. Alexandropoulos, M. Debbah, and C. Yuen, “Reconfigurable intelligent surfaces for energy efficiency in wireless communication,” IEEE Trans. Wireless Commun., vol. 18, no. 8, pp. 4157–4170, Aug. 2019.

[11] C. R. Harris et al., "Array programming with NumPy," Nature, vol. 585, pp. 357–362, 2020.

[12] P. Virtanen et al., "SciPy 1.0: Fundamental algorithms for scientific computing in Python," Nature Methods, vol. 17, pp. 261–272, 2020.
[13] J. D. Hunter, "Matplotlib: A 2D graphics environment," Computing in Science and Engineering, vol. 9, no. 3, pp. 90–95, 2007.
[14] M. Giordani, M. Polese, M. Mezzavilla, S. Rangan, and M. Zorzi, "Toward 6G networks: Use cases and technologies," IEEE Communications Magazine, vol. 58, no. 3, pp. 55–61, Mar. 2020.